The biological activities of 5,15-diaryl-10,20-dihalogeno porphyrins for photodynamic therapy

Man-Yi Li
Donghua University
Le Mi
Donghua University
Gennady Meerovich
General Physics Institute of Russian Academy of Sciences
Thin Wut Soe
University of Yangon
Ting Chen
Donghua University
Ni-Ni Than
University of Yangon
Yi-Jia Yan
Donghua University
Zhi-Long Chen (zlchen1967@qq.com)
Donghua University https://orcid.org/0000-0001-9716-8368

Research Article

Keywords: Photodynamic therapy, photosensitizer, halogenated porphyrin, anti-tumor

Posted Date: March 28th, 2022

DOI: https://doi.org/10.21203/rs.3.rs-1460073/v1

Abstract

Purpose Esophageal cancer is the most common gastrointestinal tumor and is difficult to be eradicated with conventional treatment. Porphyrin-based photosensitizers (PSs) mediated photodynamic therapy (PDT) could kill tumor cells with less damage to normal cells. As the most widely used porphyrin-based photosensitizer in clinics, Photofrin II has excellent anti-tumor effect. However, it has some disadvantages such as weak absorption at near infrared region, the complexity of components and prolonged skin photosensitivity. Here series novel 5,15-diaryl-10,20-dihalogeno porphyrin derivatives were afforded and evaluated to develop more effective and safer photosensitizers for tumor therapy.

Methods The photophysical properties and singlet oxygen generation rates of 5,15-diaryl-10,20-dihalogeno porphyrins (**I_{1-6}**, **II_{1-4}**) were tested. The cytotoxicity of **I_{1-6}** and **II_{1-4}** were measured by MTT assay. The pathway of cell death was studied by flow cytometry. *In vivo* photodynamic efficacy of **I_3** and **II_{2-4}** in Eca-109 tumor-bearing BABL/c nude mice were measured and histopathological analysis were examined.

Results 5,15-Diaryl-10,20-dihalogeno porphyrins **I_{1-6}** and **II_{1-4}** were synthesized. The longest absorption wavelength of these halogenated porphyrins (λ_{max} = 660 nm) displayed a red shift around 30 nm compared to the unhalogenated porphyrins **PS_1** (λ_{max} = 630 nm). The singlet oxygen generation rates of **I_{1-6}** and **II_{1-4}** were significantly higher than **PS_1** and HMME. All PSs mediated PDT showed obvious cytotoxic effect against Eca-109 cells compared to HMME *in vitro* and *in vivo*. Among these PSs, **II_4** exhibited appropriate absorption in the phototherapeutic window, higher $^1O_2$ generation rate (k = 0.0061 s^{-1}), the strongest phototoxicity (IC_{50} = 0.4 μM), lower dark toxicity *in vitro* on Eca-109 cells and excellent photodynamic anti-tumor efficacy *in vivo*. Besides, cell necrosis was induced by compound **II_4** mediated PDT.

Conclusion All new compounds have obvious photodynamic anti-esophageal cancer effects. Among them, the photosensitizer **II_4** showed excellent efficacy *in vitro* and *in vivo*, which has the potential to become a photodynamic anti-tumor drug.

Introduction

Esophageal cancer (Eca) is the common type of cancer and the leading cause of cancer deaths worldwide according to GLOBOCAN 2018. More than 570,000 people are newly diagnosed with esophageal carcinoma, and over 500,000 deaths are recorded annually (Bray et al. 2018; Uhlenhopp et al. 2020). PDT is a clinically approved novel method for the treatment of this cancer with many advantages including prominent selectivity, flexibility, minimum injury, and negligible toxicity to normal tissues (Wu et al. 2020). Exogenous light could activate the PSs from ground state to excited state whose energy could be transferred to surrounding ground oxygen to generate reactive oxygen species (ROS), such as singlet

oxygen ($^1O_2$), which in turn could cause oxidative damage and kill cancer cells by reacting with biomolecules (Wu et al. 2020; Li et al. 2021; Du et al. 2021; Li et al. 2021; Ormond et al. 2013).

Porphyrin, also called the “color of life”, has drawn considerable attention in photodynamic therapy, cancer diagnosis, optoelectronic materials and other aspects because of its unique physical and chemical properties (Yu et al. 2020). Currently, as the representatives of porphyrin-based photosensitizers, Photofrin II and Hematoporphyrin monomethyl Ether (HMME) are commonly used in photodynamic therapy (Massiot et al. 2018; Li et al. 2020; Zhu et al. 2018, Liao et al. 2016). Photofrin II is the first commercially available and most widely used photosensitizer due to its excellent anti-tumor effect. However, its clinical application is limited by the complexity of components and the prolonged skin photosensitivity (Li et al. 2021). HMME, developed by our group, possesses a pair of isomers which has been clinically used for the treatment of nevus flammeus and tumors. The photophysical and photochemical properties of photofrin II and HMME, such as the absorption ability at red light region, the $^1O_2$ generation ability and the photodynamic effects, is still needed to be improved to develop more effective and safer photosensitizers for tumor therapy.

Among the porphyrin derivatives, numerous researches on *meso*-tetraarylporphyrins (Cerqueira et al. 2017) have been carried out. However, only very few studies were reported about *meso*-diarylporphyrins, namely 5,15-diarylporphyrins. The preliminary study was proceeded by Banfi et al. (2006) and Wiehe et al. (2001) showed that 5,15-diarylporphyrins exhibited significantly higher photocytotoxicity than Photofrin II. The dicationic 5,15-bis-[4-(3-trimethylammoniopropyloxy)phenyl] porphyrin (XF-73) was developed for the treatment of Methicillin-resistant *Staphylococcus aureus* (MRSA) infections with satisfactory efficacy, safety and tolerability in clinical trials (Maisch et al. 2005).

Constant and abundant amino acids supply is required for tumor survival to support numerous biochemical reactions, and for tumor proliferation to synthesize structural and functional proteins (Martinez-Outschoorn et al. 2017; Hosios et al. 2016). The approval of Talaporfin (Laserphyrin®) which is the novel photosensitizer obtained by coupling chlorin e6 with aspartic acid proves that the introduction of amino acids into porphyrin-based derivatives is an effective strategy to improve the hydrophilicity and the biocompatibility (Kwitniewski et al. 2009; Serra et al. 2010; Tamiaki et al. 2014; Wang et al. 2008; Allison et al. 2004). A series of chlorin p6-based water-soluble amino acid derivatives were synthesized by Meng et al (2016), and it was found that the aqueous solubility of aspartylchlorin p6 dimethylester was significantly better than its lead compound chlorin p6 dimethylester.

In the present study, 5,15-diaryl-10,20-dihalogeno porphyrins $\mathbf{I}_{1-6}$ and $\mathbf{II}_{1-4}$ were synthesized by introducing halogen atoms and amino acids groups into 5,15-diarylporphyrins, and their photodynamic activities *in vitro* and *in vivo* against esophageal cancer were investigated (Fig. 1).

Materials And Methods

Materials

5,15-Diaryl-10,20-dihalogeno porphyrins ($\mathbf{I_{1-6}}$, $\mathbf{II_{1-4}}$) were synthesized in our laboratory (Fig. 2). All solvents and reagents were purchased from commercial suppliers and dichloromethane was used after further redistillation. HMME was donated by Shanghai Xianhui Pharmaceutical Co. Ltd. Thin-layer chromatography (TLC) analysis was carried out on silica gel plates GF254 and column chromatography was performed on silica gel (300–400 mesh). ^{1}H NMR and ^{13}C NMR spectra were recorded on a Bruker 400 MHz or 600 MHz spectrometer. MALDI-TOF mass spectra were recorded using a JEOL JMS-S3000 Spiral-TOFMS (JEOL, Tokyo, Japan). UV-vis absorption spectra were recorded on an UV-vis spectrophotometer (Jasco Model V-530, Japan). Fluorescence spectra were measured on a fluorescence spectrophotometer (FluoroMax-4, France). The geometry optimization of $\mathbf{PS_1}$, $\mathbf{I_2}$, $\mathbf{I_5}$ and $\mathbf{I_6}$ in the DMSO was carried out by DFT calculations using the B3LYP functional with a 6-31G basis set for carbon, hydrogen, nitrogen, oxygen, chlorine, bromine atoms and LANL2DZ for iodine atoms. Graphics were prepared by OriginPro 9.0 and GraphPad Prism 8. All results were presented as mean ± SD. Comparison among the groups was determined by one-way ANOVA followed by Bonferroni correction for multiple testing. $P < 0.05$ was considered statistically significant.

Density functional theory (DFT) studies

The geometry optimization of the compounds ($\mathbf{PS_1}$, $\mathbf{I_2}$, $\mathbf{I_5}$, $\mathbf{I_6}$) in DMSO was carried out by DFT calculations using the B3LYP functional with a 6-31G basis set for carbon, hydrogen, nitrogen, oxygen, chlorine, bromine atoms and LANL2DZ for iodine atoms. And then the FMOs of HOMO and LUMO energy (eV) level for the optimized structure of the products were calculated to evaluate the influence of the halogen atoms (Zhao et al. 2021).

Photophysical properties

UV-vis absorption spectra of all PSs in DMSO were recorded on an ultraviolet visible spectrophotometer (Jasco Model V-530, Japan) at wavelengths from 300 to 800 nm. Fluorescence spectra were carried out using a fluorescence spectrometer (FluoroMax-4, France) in the range 500–800 nm using 425 nm excitation wavelength. All the measurements were carried out at room temperature.

Singlet oxygen generation

1,3-Diphenylisobenzofuran (DPBF) supplied by J&K Scientific was used for the detection of the singlet oxygen generation of PSs. Generally, 3 mL portions of DMF solution containing 30 μM DPBF and 1 μM PSs were placed in a sealed quartz cuvette and irradiated with 650 nm light (CNI MRL-III-650, China) at the 5 mW/cm^2 laser intensity. The absorbance of the solution at 416 nm was measured every 10 seconds for an 80 seconds period with an ultraviolet visible spectrophotometer (Le et al. 2021; Durmuş et al. 2009). The natural logarithm values of absorption of DPBF at 416 nm were plotted against the irradiation time and fitted by a first-order linear least squares model to get the singlet oxygen generation rate of the photosensitized process (Zhang et al. 2014; Wolfgang et al. 1998). The rate of singlet oxygen generation was calculated by the following equation (Tang et al. 2005).

$$\ln([DPBF]_t / [DPBF]_0) = -kt$$

Where $[DPBF]_t$ and $[DPBF]_0$ respectively is the absorbance of DPBF after and prior irradiation. Values of *k* are singlet oxygen generation rates and *t* represent light duration.

In vitro **photosensitizing efficacy**

Cell lines and culture conditions

Human esophageal cancer cell line Eca-109 was obtained from the Type Culture Collection of the Chinese Academy of Sciences. All cell culture reagents were purchased from MesGen Biotech (Shanghai, China). Cells were cultured in normal RPMI-1640 culture medium with 10% fetal bovine serum (FBS), 50 units per mL penicillin and 50 mg mL^{-1} streptomycin in 5% CO_2 at 37°C.

Cytotoxicity

The dark- and photocytotoxicity of PSs were analyzed in Eca-109 cells following the procedures as described in the literature (Tang et al. 2005). Eca-109 cells were cultured in RPMI-1640 medium with 10% (v/v) FBS, collected with 0.25% (w/v) trypsin, and seeded in 96-well plates at 5×10^4 cells per well. The cells were allowed to attach to the bottom of the wells for 24 h prior to starting the experiment. RPMI-1640 medium containing $\mathbf{I_{1-6}}$ and $\mathbf{II_{1-4}}$ in different concentrations (range from 0 to 30 μM) was administered to cells, and allowed to uptake for 24 h, and irradiated with different light doses (0, 2, 4, 8, 12 J/cm^2) using an Nd: YAG laser at 650 nm. Non-irradiated cells were used to investigate the dark cytotoxicity. After treatment, the cell viability was determined by adding 3-(4,5-dimethyl-2-thiazolyl)-2,5-diphenyl-2H-terazolium bromide (MTT) solution (5 μg/mL in PBS) for 4 h at 37°C. Subsequently, the MTT solution was removed and 150 μL DMSO was added. The samples were shaken for 10 min at room temperature and their absorbance was measured by the microplate reader at 570 nm.

Flow cytometry analysis

Flow cytometry analysis was conducted using Annexin V-EGFP/PI Apoptosis Detection Kit (KeyGEN BioTECH, China) following the manufacturer's protocol. Briefly, Eca-109 cells were seeded in a six-well plate and incubated with the compounds at the concentration of 4 μM for 24 h and then irradiated with a light dose of 2 J/cm^2 (λ = 650 nm), followed by incubation for 6 h at 37°C. After the treatment, the media and cells were collected for each sample. The cells were resuspended with Binding Buffer in a 12×75 test tube, and then 5 μL of Annexin V and 5 μL of PI Staining Solution were added to each tube followed by incubation for 20 min at room temperature in the dark. The fluorescence of the cells was immediately determined by BD FACS Calibur Flow cytometer (Franklin Lakes, NJ).

Different PSs mediated PDT in vivo

Animals model

The BALB/c nude mice (female, 18–20 g) were obtained from Shanghai SLAC Laboratory Animal Company and housed in an air-conditioned room at 23 ± 2°C with dedicated pathogen-free barrier

facilities. For the establishment of tumor model, the 5×10^6 Eca-109 cells in 1 mL PBS were subcutaneously injected into the right region of BALB/c mice. When tumors reached a volume range from 100–150 mm^3, the following experiments were carried out. All animal procedures were performed according to the Guidelines of the Laboratory Protocol of Animal Handling and with approval from the Animal Care and Use Committee of Donghua University.

In vivo photosensitizing efficacy

The tumor xenograft mice were randomly divided into the following groups of five each: (1) Control, (2) 120 J/cm^2 light alone, (3) 2 mg/kg HMME + 120 J/cm^2 light, (4) 2 mg/kg **I_3** + 120 J/cm^2 light, (5) 2 mg/kg **II_2** + 120 J/cm^2 light, (6) 2 mg/kg **II_3** + 120 J/cm^2 light, (7) 2 mg/kg **II_4** + 120 J/ cm^2 light. The control mice were injected with the same dose of PBS. At 5 min after of the caudal vein injection, the mice were exposed to the indicated dose of light. The length (L) and width (W) of tumors were measured every other day. The tumor volume was calculated using the formula: $V = L \times W^2 \times 0.5$. After 14 days post-treatment, the mice were sacrificed and the tumors were removed and weighed.

Histological analysis

After 1 day-post treatment, tumor tissues from different groups were fixed with 4% Paraformaldehyde Fix Solution for 24 h, dehydrated through graded alcohols, and embedded in paraffin. The paraffin-embedded sections (6 μm thick) were stained with hematoxylin and eosin (H&E). Histopathological changes were observed under a light microscope (Nikon E600, Japan).

Results

Chemistry

5,15-Diaryl-10,20-dihalogeno porphyrins **I_{1-6}** were obtained by halogenation and hydrolysis of porphyrins synthesized by standard Lindsey protocol in 30%-50% total yields, as shown in **Scheme S1** (Vinogradova et al. 2009). The synthesis of 5,15-diaryl-10,20-dibromoporphyrins (**II_{1-4}**) was shown in **Scheme S2**. An amide condensation reaction occurred among compounds (**I_1**, **I_2**) and amino-acid esters. The compounds (**4a-d**) were hydrolyzed to give the target compounds (**II_{1-4}**) in 56%-70% total yields. The structures of these porphyrins (**I_{1-6}**, **II_{1-4}**) were characterized by ^{1}H NMR, ^{13}C NMR and HR-MS (**Figure. S1-25**).

Density functional theory (DFT) studies

In general, a smaller gap of HOMO and LUMO energy level (ΔE) corresponds to a stronger driving force toward the electron-transfer state. Frontier molecular orbitals (FMOs) of the HOMO and LUMO energy (eV) levels for the optimized structures of **PS_1**, **I_2**, **I_5** and **I_6** (Fig. 3) were calculated. According to our DFT calculations, ΔE of compounds **I_2** (0.09637 eV), **I_5** (0.09675 eV) and **I_6** (0.09400 eV) were smaller than compound **PS_1** (0.10184 eV) due to the existence of halogen atoms (Fig. 2). In addition, it was observed

that their corresponding ΔE values decreased with the increase of relative atomic mass of halogen atoms of *meso*-substituents.

Photophysical properties

The UV-vis absorption spectrum of the 5,15-diaryl-10,20-dihalogeno porphyrins ($\mathbf{I_{1-6}}$ and $\mathbf{II_{1-4}}$) in DMSO were presented in Fig. 4A. All compounds exhibited an intense B band at ~ 425 nm, and four Q bands at around 523 nm, 558 nm, 602 nm and 660 nm. Among these compounds, $\mathbf{I_6}$ showed the longest absorption wavelength at 664 nm. The unhalogenated porphyrins $\mathbf{PS_1}$ had fluorescence while 5,15-diaryl-10,20-dihalogeno porphyrins ($\mathbf{I_{1-6}}$ and $\mathbf{II_{1-4}}$) have no fluorescence (Fig. 4B).

Singlet oxygen generation

To evaluate the ability to produce singlet oxygen, 1,3-diphenylisobenzofuran (DPBF) was used as the quencher. The generation rate of singlet oxygen was measured by monitoring the decrease in absorbance at 415 nm with regular intervals of 10 s upon irradiation with 650 nm laser light. As shown in Fig. 5A, decomposition of DPBF did not occur in the absence of singlet oxygen. The representative halogenated porphyrins ($\mathbf{I_2}$, $\mathbf{I_6}$, $\mathbf{II_4}$) were irradiated with 650 nm laser and their absorbance did not decrease with the increase of irradiation time, which indicated that halogenated porphyrins had good photostability. Time-dependent changes of the absorption spectra of various PSs containing DPBF under light irradiation were shown in Fig. 5B, 5C and **Figure S26**. The singlet oxygen generation rates of all halogeno compounds were summarized in Table 1. The results showed that the ability of singlet oxygen generation of halogenated porphyrins was significantly higher than that of unhalogenated porphyrins $\mathbf{PS_1}$and HMME.

Table 1
Singlet oxygen generation rate of compounds $\mathbf{I_{1-6}}$, $\mathbf{II_{1-4}}$

Compound	$k\times10^{-2}(s^{-1})$	Compound	$k\times10^{-2}(s^{-1})$
$\mathbf{I_1}$	0.27	$\mathbf{II_1}$	0.29
$\mathbf{I_2}$	0.60	$\mathbf{II_2}$	0.43
$\mathbf{I_3}$	0.16	$\mathbf{II_3}$	0.30
$\mathbf{I_4}$	0.64	$\mathbf{II_4}$	0.61
$\mathbf{I_5}$	0.68	$\mathbf{PS_1}$	0.014
$\mathbf{I_6}$	0.64	**HMME**	0.026

In vitro **photosensitizing efficacy**

MTT assays were used to test the *in vitro* cytotoxicity of the target compounds against Eca-109 cells. As shown in Fig. 6A and Table 2, the cell viabilities after the treatment with compounds $\mathbf{I_{3-4}}$, and $\mathbf{II_{1-4}}$ at 10

μM were higher than 80% under dark condition while other compounds were lower than 80% under the same conditions, which suggested that compounds **I_{3-4}**, and **II_{1-4}** had negligible dark cytotoxicity. There was little difference between the IC_{50} values of halogenated porphyrins (**I_2**, **I_5** and **I_6**) with Cl, Br and I under dark or light irradiation, as shown in **Figure S27**. The IC_{50} values of all target compounds were evidently smaller than HMME under light irradiation of 12 J/cm^2 (Table 2). It was noteworthy that significant decrease in cell viability of Eca-109 cells after the treatment with compounds **I_{1-3}**, **I_{5-6}**, and **II_{1-4}** at concentration of 4 μM and a light dose of 12 J/cm^2 was observed (**Figure S27** and Fig. 6B), which indicated that these compounds had obvious photodynamic activities against Eca-109 cells.

Table 2
IC_{50} values of **I_{1-6}**, **II_{1-4}** in Eca-109 cells upon different light dose irradiation

Compound	IC_{50} (μM)				
	0 J/cm^2	2 J/cm^2	4 J/cm^2	8 J/cm^2	12 J/cm^2
I_1	11.1	8.1	6.2	4.6	3.5
I_2	23.4	7.6	4.8	3.9	3.0
I_3	28.6	4.6	3.9	3.2	2.4
I_4	> 30	> 30	23.3	14.0	7.7
I_5	22.2	20.0	5.8	3.7	2.9
I_6	16.5	10.0	6.4	3.8	2.5
II_1	26.6	13.8	7.2	4.1	2.2
II_2	26.3	4.9	2.7	1.9	0.9
II_3	> 30	5.4	4.2	3.4	1.6
II_4	24.4	3.9	1.9	1.6	0.4
HMME	27.9	22.4	18.6	15.0	9.2

Flow cytometry analysis

To investigate the cell death induced by different PSs, Eca-109 cells after PDT were incubated for 5 h and stained with the V-FITC/PI apoptosis assay kit for flow cytometry analysis. As shown in Fig. 7, no necrotic cells were detected in the control group. After 5 h post-PDT, the proportion of living cells were decreased in all PDT-treatment groups, especially dropped to 48.40% and 45.58% in **I_3** and **II_4** groups respectively. **II_4**-PDT mainly induced cell necrosis, while **I_3**-PDT could induce cell necrosis and apoptotic.

Different PSs mediated PDT in vivo

Since compounds **I_3**, **II_2**, **II_3** and **II_4** had more obvious photodynamic cytotoxicity than others under the same conditions, their photodynamic efficacy in Eca-109 tumor-bearing BABL/c nude mice were evaluated. The compounds at a dose of 2 mg/kg were injected intravenously into mice, followed by irradiation of 120 J/cm^2 light at tumor site for single time. As shown in Fig. 8A, 8B and 8C, almost negligible inhibition of tumor growth was observed from the mice treated with light only. Notably, **II_2** and **II_4** showed more prominent anti-tumor PDT effect compared to the control group, light group and HMME group, especially **II_4**.

After 1-day post treatment, the tumor tissue sections were separated then stained with hematoxylin and eosin (H&E) reagent. As shown in Fig. 8D, significant tumor tissue damage in the PDT group could be observed under microscopy compared to the control group. The results of the tumor growth curve and histological examination showed that **II_4** had the best photodynamic antitumor activity *in vivo*.

Discussion And Conclusion

In this study, series novel photosensitizers were prepared and their photodynamic activities were investigated. The longest absorption wavelength of halogenated porphyrins was superior to unhalogenated porphyrins as shown in Fig. 4, which was correlated with their small ΔE calculated by the DFT. It is interesting that all halogenated porphyrins showed no fluorescence emission, which is caused by the corresponding smaller ΔE values to transfer most of the first excited state populations of PSs into triplet excited state. In addition, as shown in Table 1, the singlet oxygen generation rates of all halogeno compounds were remarkably higher than **PS_1** and HMME, because the increase of the triplet excited state populations of halogenated porphyrins was beneficial to the generation of singlet oxygen. The singlet oxygen generation rates of porphyrin-amino acid conjugates have been improved to a certain extent, especially bromoporphyrins linked with 5-aminolevulinic acid (**II_2**, **II_4**). However, the singlet oxygen generation rates of bromoporphyrin (**I_2**), chloroporphyrin (**I_5**) and iodoporphyrin (**I_6**) are slightly different. It was also showed that all compounds (**I_{1-6}** and **II_{1-4}**) had more obvious photodynamic anti- Eca-109 cell activities *in vitro* than compounds HMME at the same treatment conditions, and the compounds **I_{3-4}**, **II_{1-4}** had negligible dark cytotoxicity. Moreover, with 12 J/cm^2 irradiation of 650 nm laser, compounds **II_4** at 4 μM had the excellent anti-tumor effect and low dark toxicity *in vitro*. **II_4**-PDT mainly induced cell necrosis, while **I_3**-PDT could induce cell necrosis and apoptotic (Fig. 7). Notably, compound **II_4** showed more prominent anti-tumor photodynamic efficacy in Eca-109 tumor-bearing BABL/c nude mice (Fig. 8).

In summary, **II_4** linked with 5-aminolevulinic acid showed excellent photodynamic efficacy on Eca-109 cells *in vitro* and *in vivo*, which has the potential to act as a photodynamic anti-tumor drug.

Abbreviations

PDT: Photodynamic therapy

PSs: Photosensitizers

ROS: Reactive oxygen species

$^1O_2$: Singlet oxygen

ISC: Intersystem crossing

DFT: Density functional theory

TLC: Thin Layer Chromatography

NMR: Nuclear magnetic resonance

MS: Mass spectra

FMOs: Frontier molecular orbitals

HMME: Hematoporphyrinmonomethyl ether

DMSO: Dimethyl sulfoxide

DMF: Dimethylformamide

DPBF: 1,3-Diphenylisobenzofuran

DDQ: 2,3-Dicyano-5,6-dichlorobenzoquinone

H&E reagent: Hematoxylin-eosin reagent

FBS: Fetal bovine serum

PBS: Phosphate buffered saline

MTT: 3-(4,5-Dimethyl-2-thiazolyl)-2,5-diphenyl-2Hterazolium bromide

Declarations

Acknowledgments

This work was supported by the National Natural Science Foundation of China (No. 21977016), Foundation of Shanghai Science and Technology Committee (No. 19410711000, 20430730900, 20490740400, 21430730100) and Foundation of Science and Technology Commission of Pudong New Area (No. PKJ2019-Y31, PKJ2020-Y42).

Conflict of interest

The authors have declared no conflict of interest.

Author Contributions

The manuscript was written through contributions of all authors. All authors have read

and agreed to the final version of the manuscript.

References

1. Bray F, Ferlay J, Jemal A et al (2018) Global cancer statistics 2018: GLOBOCAN estimates of incidence and mortality worldwide for 36 cancers in 185 countries. CA Cancer J Clin 68(6):394–424. https://doi.org/10.3322/caac.21492
2. Uhlenhopp DJ, Then EO, Gaduputi V et al (2020) Epidemiology of esophageal cancer: update in global trends, etiology and risk factors. Clin J Gastroenterol 13(6):1010–1021. https://doi.org/10.1007/s12328-020-01237-x
3. Wu J, Sha J, Wang P et al (2020) Recent advances in theranostic agents based on natural products for photodynamic and sonodynamic therapy. View 1(3):20200090. https://doi.org/10.1002/VIW.20200090
4. Li J, Ou H, Ding D et al (2021) Recent progress in boosted PDT induced immunogenic cell death for tumor immunotherapy. Chem Res Chin Univ 37(1):83–89. https://doi.org/10.1007/s40242-021-0402-5
5. Du J, Shi T, Peng X et al (2021) Enhanced photodynamic therapy for overcoming tumor hypoxia: From microenvironment regulation to photosensitizer innovation. Coordin Chem Rev 427(6):213604. https://doi.org/10.1016/j.ccr.2020.213604
6. Li MY, Gao YH, Chen ZL et al (2021) Synthesis and evaluation of novel fluorinated hematoporphyrin ether derivatives for photodynamic therapy. Bioorg Chem 107:104528. https://doi.org/10.1016/j.bioorg.2020.104528
7. Ormond AB, Freeman HS et al (2013) Dye sensitizers for photodynamic therapy. Mater (Basel) 6(3):817–840. https://doi.org/10.3390/ma6030817
8. Yu WM, Zhen WQ, Liu YM et al (2020) Porphyrin-based metal-organic framework compounds as promising nanomedicines in photodynamic therapy. ChemMedChem 15:1766–1775. https://doi.org/10.1002/cmdc.202000353
9. Massiot J, Rosilio V, Makky A et al (2018) Newly synthesized lipid-porphyrin conjugates: evaluation of their self-assembling properties, their miscibility with phospholipids and their photodynamic activity in vitro. Chemistry 24(72):19179–19194. https://doi.org/10.1002/chem.201804865
10. Li X, Lovell JF, Chen X et al (2020) Clinical development and potential of photothermal and photodynamic therapies for cancer. Nat Rev Clin Oncol 17(11):657–674.

https://doi.org/10.1038/s41571-020-0410-2

11. Zhu W, Gao YH, Chen ZL et al (2018) Comparison between porphin, chlorin and bacteriochlorin derivatives for photodynamic therapy: Synthesis, photophysical properties, and biological activity. Eur J Med Chem 160:146–156. https://doi.org/10.1016/j.ejmech.2018.10.005
12. Liao PY, Wang XR, Chen ZL et al (2017) Synthesis of 2-morpholine tetraphenylporphyrins and their photodynamic activities. Bioorg Chem 71:299–304. https://doi.org/ 10.1016/j.bioorg.2017.02.015
13. Chatterjee T, Shetti VS, Ravikanthet M et al (2017) Heteroatom-containing porphyrin analogues. Chem Rev 117:3254–3328. https://doi.org/10.1021/acs.chemrev.6b00496
14. Banfi S, Caruso E, Gramatica P et al (2006) Comparison between 5,10,15,20-tetraaryl- and 5,15-diarylporphyrins as photosensitizers: synthesis, photodynamic activity, and quantitative structure-activity relationship modeling. J Med Chem 49(11):3293–3304. https://doi.org/10.1021/jm050997m
15. Wiehe A, Simonenko EJ, RÖDer B et al (2001) Hydrophilicity vs hydrophobicity - varying the amphiphilic structure of porphyrins related to the photosensitizer m-THPC. J Porphyr and Phthalocya 5(10):758–761. https://doi.org/10.1002/jpp.389
16. Maisch T, Bosl C, Abels C et al (2005) Photodynamic effects of novel XF porphyrin derivatives on prokaryotic and eukaryotic cells. Antimicrob Agents Chemother 49(4):1542–1552. https://doi.org/10.1128/AAC.49.4.1542-1552.2005
17. Jeong HG, Choi MS et al (2016) Design and properties of porphyrin-based singlet oxygen generator. Isr J Chem 56:110–118. https://doi.org/10.1002/ijch.201500026
18. Martinez-Outschoorn UE, Peiris-Pages M, Lisanti MP et al (2017) Cancer metabolism: a therapeutic perspective. Nat Rev Clin Oncol 14(1):11–31. https://doi.org/10.1038/ nrclinonc.2017.1
19. Hosios AM, Hecht VC, Vanderheiden M et al (2016) Amino acids rather than glucose account for the majority of cell mass in proliferating mammalian cells. Dev Cell 36(5):540–549. https://doi.org/10.1016/j.devcel.2016.02.012
20. Kwitniewski M, Juzeniene A, Moan J et al (2009) Diamino acid derivatives of PpIX as potential photosensitizers for photodynamic therapy of squamous cell carcinoma and prostate cancer: In vitro studies. J Photoch and Photobio B: Biology 94(3):214–222. https://doi.org/10.1016/j.jphotobiol.2008.11.005
21. Serra VV, Zamarrón A, Sanz-Rodríguez F et al (2010) New porphyrin amino acid conjugates: Synthesis and photodynamic effect in human epithelial cells. Bioorg Med Chem 18(16):6170–6178. https://doi.org/10.1016/j.bmc.2010.06.030
22. Tamiaki H, Isoda Y, Machida S et al (2014) Synthesis of chlorophyll-amino acid conjugates as models for modification of proteins with chromo/fluorophores. Bioorg Med Chem 22(4):1421–1428. https://doi.org/10.1016/j.bmc.2013.12.059
23. Wang HM, Jiang JQ, Liu XY et al (2008) Porphyrin with amino acid moieties: A tumor photosensitizer. Chem Biol Interact 172(2):154–158. https://doi.org/10.1016/j.cbi. 2007.11.016
24. Allison RR, Downie GH, Sibata CH et al (2004) Photosensitizers in clinical PDT. Photodiagn Photodyn 1(1):27–42. https://doi.org/10.1016/S1572-1000(04)00007-9

25. Meng Z, Yu B, Yao J et al (2016) Chlorin p6-based water-soluble amino acid derivatives as potent photosensitizers for photodynamic therapy. J Med Chem 59(10):4999–5010. https://doi.org/10.1021/acs.jmedchem.6b00352
26. Zhao X, Yao Q et al (2021) An approach to developing cyanines with simultaneous intersystem crossing enhancement and excited-state lifetime elongation for photodynamic antitumor metastasis. J Am Chem Soc 143:12345–12354. https://doi.org/10.1021/jacs.1c06275
27. Le NA, Babu V, Spingler B et al (2021) Photostable Platinated Bacteriochlorins as Potent Photodynamic Agents. J Med Chem 64(10):6792–6801. https://doi.org/10.1021/acs.jmedchem.1c00052
28. Durmuş M, Erdoğmuş A, Nyokong T et al (2009) The synthesis and photophysicochemical behaviour of novel water-soluble cationic indium(III) phthalocyanine. Dyes Pigm 82(2):244–250. https://doi.org/10.1016/j.dyepig.200901.008
29. Zhang LJ, Bian J, Chen ZL et al (2014) Photosensitizing effectiveness of a novel chlorin-based photosensitizer for photodynamic therapy in vitro and in vivo. J Cancer Res Clin Oncol 140(9):1527–1536. https://doi.org/10.1007/s00432-014-1717-0
30. Wolfgang, Spiller, Röder, et al. (1998) Singlet oxygen quantum yields of different photosensitizers in polar solvents and micellar solutions. J Porphyr Phthalocya 2 (2): 145 - 158. https://doi.org/10.1002/(SICI)1099-1409(199803/04)2:2<145::AID-JPP60> 3.0.C
31. W. Tang, H. Xu, R. Kopelman, et al. (2005) Photodynamic characterization and in vitro application of methylene blue-containing nanoparticle platforms, Photochem Photobiol, 81: 242-249. https://doi.org/10.1562/2004-05-24-ra-176.1
32. EV Vinogradova, YY Enakieva, AY Tsivadze, et al. (2009) Synthesis of meso-substituted porphyrins as precursors in creating highly ordered electroluminescent polymer materials. Prot Met Phys Chem+ 45(5): 529 - 534. https://doi.org/10.1134/S2070205109050050

Figures

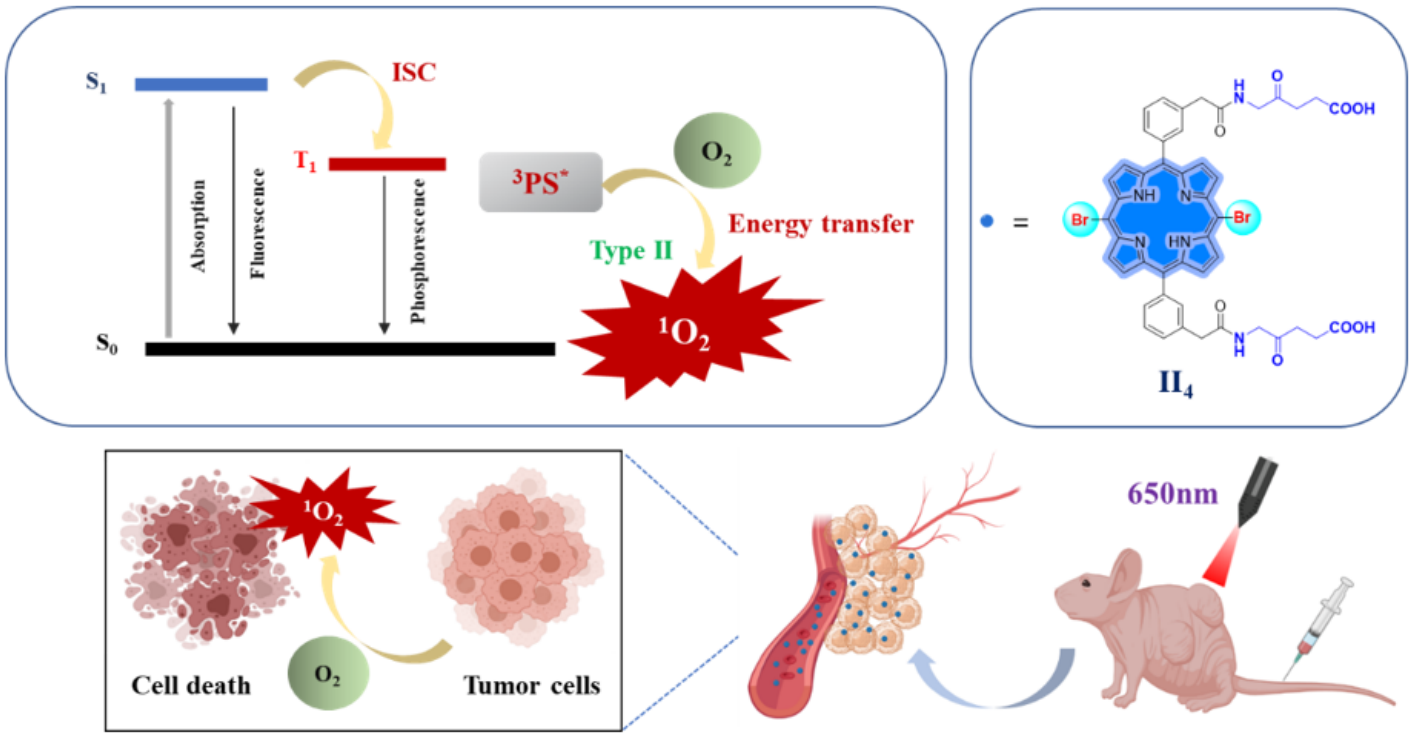

Figure 1

The schematic diagram of $\mathbf{II_4}$ mediated PDT

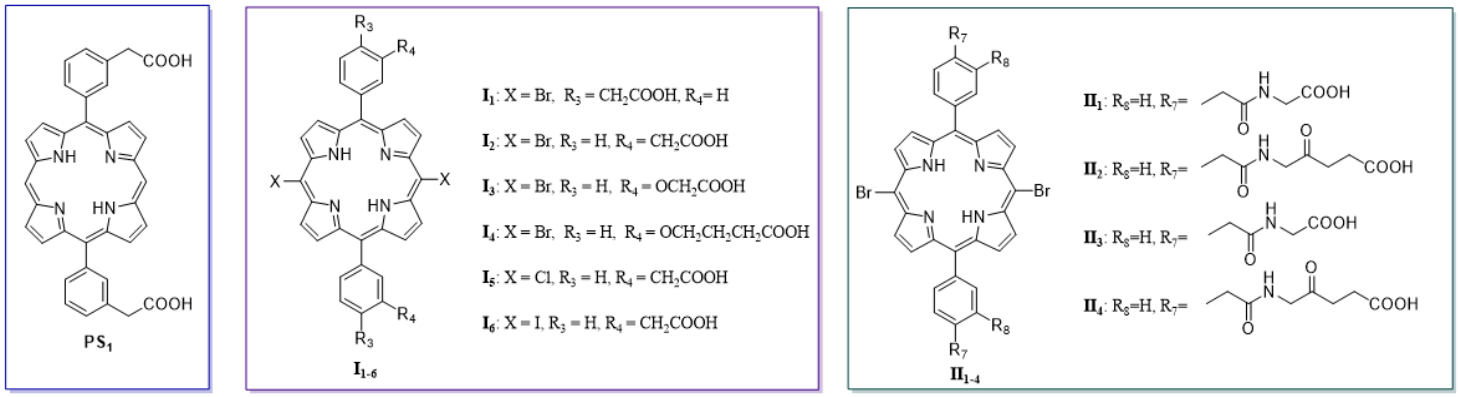

Figure 2

The structures of 5,15-diaryl-10,20-dihalogeno porphyrins ($\mathbf{I_{1\text{-}6}}$, $\mathbf{II_{1\text{-}4}}$)

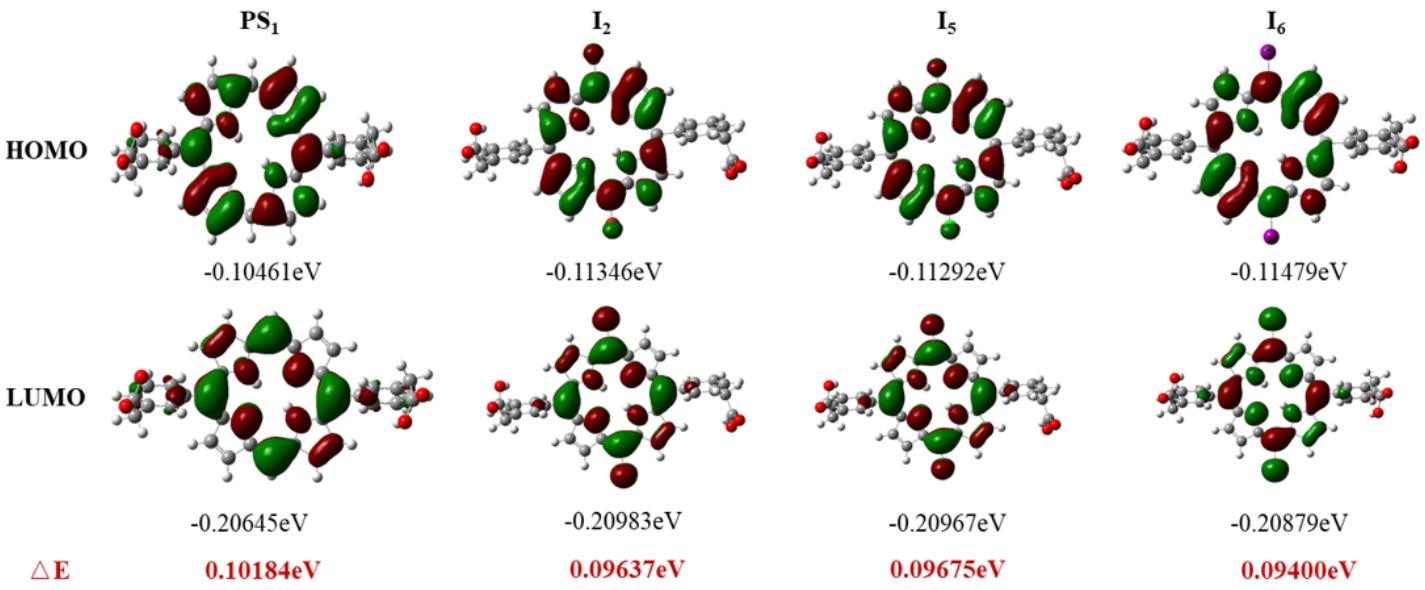

Figure 3

FMOs and ΔE of PS_1, I_2, I_5, I_6

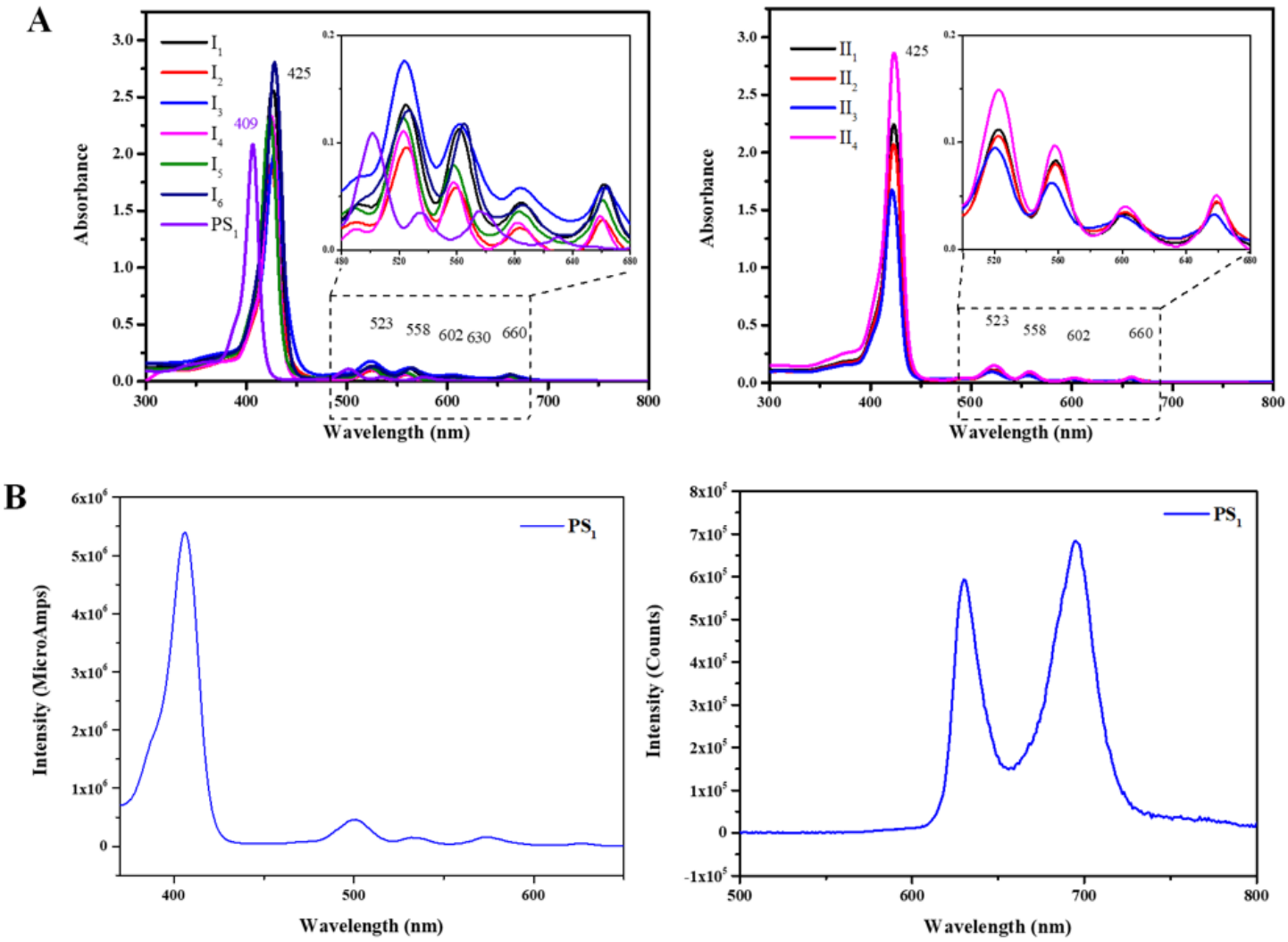

Figure 4

The spectrum properties of compounds. **A** UV-vis absorption spectra of compounds **PS_1**, **I_{1-6}** and **II_{1-4}** at 10 μM in DMSO. **B** Fluorescence excitation and emission spectra of compounds **PS_1** in DMSO at the concentration of 10 μM.

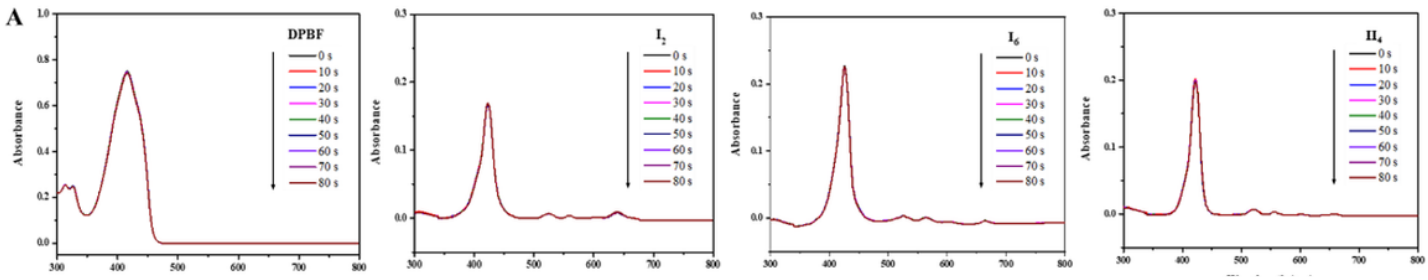

Figure 5

The singlet oxygen generation of compounds. **A** Photodegradation of DPBF and compounds **I_2**, **I_6**, **II_4** under 650 nm laser irradiation (5 mW/cm^2) every 10 seconds. **B** Photodecomposition of DPBF in the presence of **II_4** under 650 nm laser irradiation (5 mW/cm^2) every 10 seconds. **C** First-order plot for the photodecomposition of DPBF after PDT with the compounds.

Figure 6

The efficacy of compounds against Eca-109 cells *in vitro*. **A** Dark cytotoxicity of compound **$I_{1\text{-}6}$**, **$II_{1\text{-}4}$** at concentrations ranging from 0 to 30 μM in Eca-109 cells. **B** The cell viabilities treated by **II_4** at concentrations ranging from 2 to 10 μM under different light doses. Data represents mean ± SD.

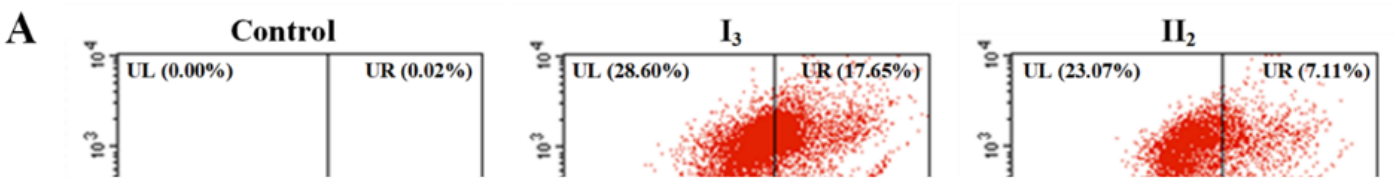

Figure 7

The extent and mode of cell death induced by different PSs-PDT. **A** Flow cytometric assay of **I_3**, **II_2**, **II_3** and **II_4** at 4 μM exposed to 2 J/cm^2 of light. LL: Annexin V (−) PI (−), lived cell; LR: Annexin V (+) PI (−), early apoptotic cells; UR: Annexin V (+) PI (+), late apoptotic cells; UL: Annexin V (−), necrotic cells. **B** Histogram of apoptotic cells, necrosis cells and live cells after the treatment. Data represents mean ± SD.

Figure 8

Evaluation of tumor growth inhibition in the Eca-109-tumor-bearing model mediated by PDT. **A** Tumor images after 14 days. **B** Tumor growth curves after different treatments. *P < 0.05, **P < 0.001, ***P <0.0001 vs HMME-PDT group. **C** Tumor weight. (D) Histological sections of tumor tissues stained with hematoxylin and eosin. Scale bar =50 μm.

Supplementary Files

This is a list of supplementary files associated with this preprint. Click to download.

- SupportingMaterial.docx